PHYSICAL REVIEW B **96**, 155118 (2017)

Periodic table for Floquet topological insulators

Rahul Roy and Fenner Harper
Department of Physics and Astronomy, University of California, Los Angeles, California 90095, USA
(Received 14 July 2016; revised manuscript received 22 February 2017; published 13 October 2017)

Dynamical phases with novel topological properties are known to arise in driven systems of free fermions. In this paper, we obtain a 'periodic table' to describe the phases of such time-dependent systems, generalizing the periodic table for static topological insulators. Using K theory, we systematically classify Floquet topological insulators from the ten Altland-Zirnbauer symmetry classes across all dimensions. We find that the static classification scheme described by a group $\mathcal{G}$ becomes $\mathcal{G}^{\times n}$ in the time-dependent case, where n is the number of physically important gaps in the quasienergy spectrum (including any gaps at quasienergy π). The factors of $\mathcal{G}$ may be interpreted as arising from the bipartite decomposition of the unitary time-evolution operator. Topologically protected edge modes may arise at the boundary between two Floquet systems, and we provide a mapping between the number of such edge modes and the topological invariant of the bulk.

DOI: 10.1103/PhysRevB.96.155118

I. INTRODUCTION

The discovery of topological insulators and the theoretical and experimental activity that it inspired has led to major advances in our understanding of zero-temperature gapped phases [1,2]. While the first new systems to be discovered were specific topological phases of insulators and superconductors in one to three dimensions [3–9], these were eventually arranged into a 'periodic table,' which extended the classification to all dimensions and symmetry classes [10]. This unifying approach revealed a remarkable underlying periodicity, using connections between K theory and Bott periodicity on the one hand, and free fermionic topological phases with symmetries on the other.

The generalized topological insulators that this classification scheme describes exhibit robust, topologically protected edge modes in the presence of a boundary and are characterized by invariant integers encoded in the topology of their wave functions. In this way, the periodic table captures the complete set of bulk-edge connections between bulk Hamiltonians and their protected edge states. Equivalently, one can interpret the periodic table as expressing the connection between the unitary time evolution of a constant Hamiltonian (evaluated after some time T), and the corresponding edge eigenstates. In this picture, the periodic table may be regarded as part of a more general framework of topological bulk-edge connections between unitary time evolution operators and protected edge modes. When the Hamiltonians involved are no longer constrained to be time independent, new types of bulk-edge connection may occur. In this paper, we seek to capture the structure of these dynamical bulk-edge connections by constructing a generalized periodic table for free fermionic systems with time-dependent Hamiltonians.

Among our motivations for studying these systems is the set of (time-periodic) Floquet topological insulators that have recently been the subject of much experimental and theoretical effort [see Refs. [11,12] for a review]. Some of these efforts have considered using periodic driving to force a system into a topological state [13–23], and significant experimental progress has been made in this direction in photonic systems [24–27] and using ultracold atoms [28,29]. Floquet states (albeit nontopological ones) have also been observed in the solid state on the surfaces of topological insulators [30,31]. Other recent work has demonstrated the possibility of generating intrinsically dynamical topological phases that cannot be realized in static systems [32–41].

Although we will make connections to Floquet theory, our approach provides a description of time-dependent topological phases in a manner that does not require time periodicity. Instead, we consider equivalence classes of unitary time-evolution operators in general and focus on the instantaneous topological edge states that might exist in a system after a particular time evolution. Our main result will be the production of a generalized periodic table of Floquet topological insulators, which may be found in Table II. In the process, we find many new Floquet topological phases that have not been considered before and provide a general and unifying description for all symmetry classes and dimensions. As in the case of (static) topological insulators, this picture provides a connection between the manifestations of Bott periodicity in K theory and the topological phases of driven free fermionic systems, describing both the strong and weak invariants of the system.

Some elements of our generalized periodic table have appeared in the context of Floquet systems elsewhere in the literature. Notably, previous work has considered dynamical topological phases in 1D chains with emergent Majorana fermions [33,35], 2D systems without symmetries [34], and driven analogues of the 2D time-reversal invariant topological insulators [39]. Topological phases of 1D chiral lattices have also been described in Ref. [36], albeit using a different definition of chiral symmetry than will be used in this work. In addition, Ref. [38] describes a band singularity approach to the characterization of Floquet topological phases, introducing new results for 3D systems with time-reversal symmetry. After the completion of our work we discovered Ref. [41], which extends the formulation of strong topological invariants for classes A and AIII to all dimensions. While our work does not rely on invariants for classification and discusses several other cases, our results seem to be consistent with these existing discussions and incorporates them into a general, unifying periodic table. Our results also capture the complete set of strong and weak topological invariants in each case.

Several other works discuss driven, 1d topological phases in the context of quantum walks [42–45]. In particular, a complete

classification of 1d quantum walks has been obtained using scattering theory [44]. These results are consistent with our classification of 1d Floquet systems, although the setting and symmetry definitions used are slightly different. In the opposite limit, time-dependent topological systems have also been studied through adiabatic cycles, where a system parameter is varied slowly while maintaining a gap in the Hamiltonian [46–50]. In Ref. [50], a classification of adiabatic pumps of this form was obtained for classes AIII and DIII. These results also agree with our classification scheme for these classes, although it should be noted that Floquet systems are generically very far from the adiabatic limit (and there is no requirement to maintain an instantaneous gap).

In this paper we consider noninteracting systems, but the ideas we outline also develop some of the intuition required for the study of interacting topological phases, a topic that has been the focus of much recent study, both by the current authors and others [51–58]. Importantly, the statements we make in the noninteracting case can, to a great extent, be made mathematically precise, while arguments for interacting systems necessarily require a certain amount of conjecture. In this way, we hope that this paper will provide a useful corroboration of the ideas introduced in Ref. [54].

The outline of this paper is as follows. In Sec. II, we introduce unitary evolution operators in the context of time-dependent systems and establish the homotopy formalism that we will require throughout the text. In Sec. III we introduce unitary loops and explain how a general unitary evolution may be deformed into a unitary loop followed by a constant Hamiltonian evolution, a theorem that is central to our approach. We go on to classify unitary loops for the Altland-Zirnbauer (AZ) symmetry classes in Sec. IV, before relating this classification scheme to general unitaries and edge modes in Sec. V. Finally, we give some concluding remarks in Sec. VI. In order to aid ease of reading, we have omitted some of the more mathematical sections from the main text. These may be found in the appendices.

II. UNITARY TIME EVOLUTION OPERATORS AND THEIR PROPERTIES

A. Time-dependent quantum systems

The aim of this paper is to classify the novel types of topological edge mode that can arise in a noninteracting quantum system after it has evolved in time due to some time-dependent Hamiltonian $H(t)$. In general, instantaneous eigenstates satisfy the time-dependent Schrödinger equation and evolve in time through the unitary transformation

$$|\psi(t)\rangle = \mathcal{T}\exp\left[-i\int_0^t H(t')\mathrm{d}t'\right]|\psi(0)\rangle \equiv U(t)|\psi(0)\rangle, \quad (1)$$

with $\mathcal{T}$ the time ordering operator. $U(t)$ is the time evolution operator, and, being unitary, has eigenvalues that lie on the unit circle in the complex plane. We write these eigenvalues as $e^{-i\epsilon(t)t}$, and focus on the instantaneous quasienergies given by $\{\epsilon(t)\}$, taken to lie in the range $-\pi/t < \epsilon(t) \leqslant \pi/t$. In a spatially periodic system, the instantaneous single-particle quasienergies form bands labeled by the momentum $\mathbf{k}$ and a band index. In some ways, these bands bear a resemblance to the ordinary bands of a (static) periodic Hamiltonian, although we will find that the periodic nature of the quasienergy spectrum generally allows for a much richer structure.

We are particularly interested in the quasienergy spectrum after evolution through some time period T, and we write the quasienergies at $t = T$ simply as ϵ. At this point, a system with an open boundary should have a similar quasienergy spectrum to the corresponding periodic system, with the possible addition of energy levels in the gaps between the bulk bands. The existence of gap states indicates the presence of topologically protected edge modes, which we aim to classify in this text.

Most previous work in this area has focused on Floquet systems: those whose time-dependent Hamiltonians satisfy $H(t+T) = H(t)$ for some time period T. In a Floquet system, we can use an analogy of Bloch's theorem to write the instantaneous eigenstates as $|\psi(t)\rangle = e^{-i\epsilon(t)t}|\phi(t)\rangle$ with $|\phi(t+T)\rangle = |\phi(t)\rangle$. In this way, after a complete time period, Floquet states simply pick up a phase, since $U(T)|\psi(0)\rangle = e^{-i\epsilon T}|\psi(0)\rangle$. It should be noted, however, that the time evolution operator $U(t)$ is generally *not* periodic, even if it is derived from a periodic Hamiltonian.

Although Floquet theory provides a useful setting in which to discuss time-dependent systems, we emphasize that our conclusions will be much more general than this. The statements we make are essentially about the topology of the space of unitary evolutions (with symmetry), and the unitary evolutions that we classify do not necessarily need to be generated by a time-periodic Hamiltonian. Instead, they may be considered as paths within the space of evolutions. The phase space of unitary evolutions is discussed in some detail in Ref. [58].

B. Particle-hole, time-reversal, and chiral symmetries

In this paper, we are concerned with free fermionic systems that fall within the symmetry classes of the AZ classification scheme [59–61]. These classes are distinguished by the presence or absence of two antiunitary symmetries and one unitary symmetry, as well as the general form of the relevant symmetry operators.

In systems with particle-hole symmetry (PHS), there exists a PHS operator $\mathcal{P} = \mathcal{K}P$, where $\mathcal{K}$ is the complex conjugation operator and P is unitary, that acts on the band Hamiltonian to give

$$PH(\mathbf{k},t)P^{-1} = -H^*(-\mathbf{k},t). \quad (2)$$

Similarly, in systems with time-reversal symmetry (TRS), there exists a TRS operator $\Theta = \mathcal{K}\theta$, where $\mathcal{K}$ is again the complex conjugation operator and θ is unitary, that acts on the band Hamiltonian to give

$$\theta H(\mathbf{k},t)\theta^{-1} = H^*(-\mathbf{k},T-t). \quad (3)$$

With this definition, we have assumed without loss of generality that $t = T/2$ is the point in time about which the Hamiltonian is symmetric.

From the definition of the time evolution operator in Eq. (1), it follows that these symmetry operators, if present, act on

TABLE I. Standard expressions for symmetry operators within each Altland-Zirnbauer (AZ) symmetry class. σ_i are the Pauli matrices and $\mathbb{I}$ is the identity.

Symmetry Operator	Cartan Label $\mathcal{S}$
$P = \sigma_1 \otimes \mathbb{I}$	BDI, D, DIII
$P = i\sigma_2 \otimes \mathbb{I}$	CII, C, CI
$\theta = \mathbb{I}$	AI, BDI, CI
$\theta = \mathbb{I} \otimes i\sigma_2$	AII, CII, DIII
$C = \sigma_3 \otimes \mathbb{I}$	AIII

$U(\mathbf{k},t)$ to give

$$PU(\mathbf{k},t)P^{-1} = U^*(-\mathbf{k},t) \tag{4}$$

$$\theta U(\mathbf{k},t)\theta^{-1} = U^*(-\mathbf{k},T-t)U^{\dagger *}(-\mathbf{k},T). \tag{5}$$

The actions of each symmetry operator on the time evolution unitary are derived in Appendix A.

If both TRS and PHS are present, there is an additional unitary symmetry $C = P\theta$ that acts on the Hamiltonian to give

$$CH(\mathbf{k},t)C^{-1} = -H(\mathbf{k},T-t). \tag{6}$$

More generally, there may be a chiral symmetry (CS) operator $C \neq P\theta$ that acts on the Hamiltonian according to Eq. (6) even in the absence of PHS and TRS. This defines the final AZ symmetry class, labeled AIII. When acting on the time evolution unitary, the CS operator gives (derived in Appendix A)

$$CU(\mathbf{k},t)C^{-1} = U(\mathbf{k},T-t)U^{\dagger}(\mathbf{k},T). \tag{7}$$

We note that our definition of chiral symmetry for periodic systems is slightly different from that used in some previous works [36,38].

After a suitable basis transformation, P, θ, and C can always be written in certain standard forms, as shown in Table I. The operators P and θ may each either square to $+\mathbb{I}$ or $-\mathbb{I}$, leading (along with the chiral symmetry operator) to ten distinct AZ symmetry classes [59–61]. We write the set of unitaries that belong to each symmetry class as $\mathcal{U}^{\mathcal{S}}$, where $\mathcal{S}$ is the appropriate Cartan label. To simplify notation, we set $T = 1$ from now on, so that $t \in [0,1]$. We will also often omit the explicit momentum and time dependence of a unitary operator $U(\mathbf{k},t)$ if the meaning is clear.

C. Gapped unitaries

We are interested in the protected edge modes that may arise in the gaps of the quasienergy spectrum at the end of a unitary evolution if the system has a boundary. For this reason, we will restrict the discussion to consider only gapped unitaries, which we define to be unitary evolutions of the form in Eq. (1), which at their end point, $U(\mathbf{k},1)$, have at least one value of quasienergy in the closed system that no bands cross [62]. Importantly, we do not require that the instantaneous quasienergy spectrum be gapped for intermediate values of t $(0 < t < 1)$. We write the set of all such gapped unitaries within the AZ symmetry class $\mathcal{S}$ as $\mathcal{U}_g^{\mathcal{S}}$ and note that a unitary evolution of this form may be represented as a continuous matrix function $U(\mathbf{k},t)$ with $0 \leqslant t \leqslant 1$ and $\mathbf{k}$ taking values within the d-dimensional Brillouin zone, which we call X. It is clear that $U(\mathbf{k},t)$ evolves from the identity matrix at $t = 0$.

The gap structure at the end of a unitary evolution will depend on the symmetry of the underlying Hamiltonian and in general can be rather complicated. A schematic example of a gapped unitary evolution with PHS is shown in Fig. 1, which emphasizes both the nontrivial evolution and the quasienergy band structure at the end point. The most commonly considered quasienergy gaps are those at $\epsilon = 0$ and $\epsilon = \pi$, since, in a system with particle-hole or chiral symmetry, these are the gaps about which the system is symmetric. In systems without these symmetries, physically relevant energy gaps may appear anywhere in the spectrum, although in these cases a generic gap can always be moved homotopically (a term we define precisely below) to $\epsilon = 0$ or $\epsilon = \pi$. For these reasons, we will assume the gaps in the spectrum occur at these points throughout the next two sections, leaving a general discussion of gap structures to Sec. V.

The gapped spectrum in Fig. 1(b) resembles the band structure of a conventional, static Hamiltonian, with two well-separated bands and a gap at zero. In this situation, it is useful to define the effective Floquet Hamiltonian H_F through

$$H_F(\mathbf{k}) = i \ln [U(\mathbf{k},1)], \tag{8}$$

where the branch cut of the logarithm can be placed in the gap at $\epsilon = \pi$. According to Eq. (1), the Floquet Hamiltonian might naively be interpreted as the effective static Hamiltonian that, under time evolution, generates the quasienergy spectrum of the corresponding unitary, $U(\mathbf{k},1)$. If the Floquet Hamiltonian is topologically nontrivial, we might expect the edge modes associated with H_F to transfer to edge modes in the quasienergy spectrum of $U(\mathbf{k},1)$. Indeed, if one considers evolution with a time-independent but topologically nontrivial Hamiltonian, then $U(\mathbf{k},1)$ for the open system will have robust edge modes if the corresponding unitary for the closed system is gapped at zero.

Although this intuition goes some way towards explaining the protected edge modes of unitary operators, the time-dependent situation is inherently more complicated: In general, there can be edge modes in the quasienergy gaps at both $\epsilon = 0$ and $\epsilon = \pi$, the latter of which lie beyond a description in terms of the effective Floquet Hamiltonian. Indeed, recent studies have demonstrated systems that exhibit edge modes in both gaps even when the effective Floquet Hamiltonian is the identity operator (see, for example, Ref. [34]). To fully characterize the edge modes of a unitary operator $U(\mathbf{k},1)$, we require information about the unitary evolution $U(\mathbf{k},t)$ throughout the period of evolution $0 \leqslant t \leqslant 1$. In Fig. 1(a) we show a nontrivial evolution of this form that might generate edge modes in the gaps at $\epsilon = 0$ and $\epsilon = \pi$. An interesting feature of Floquet systems with edge modes at $\epsilon = \pi$ is that the unitary for the open system cannot always be written in the form $U(\mathbf{k},1) = e^{-iH(\mathbf{k})}$ for some local Hamiltonian $H(\mathbf{k})$. Notably, if the system has PHS, then there is no way of shifting the modes at $\epsilon = \pi$ to $\epsilon = 0$ without breaking the symmetry. This contrasts with the closed system, whose gapped unitary can always be written in terms of a local Hamiltonian.

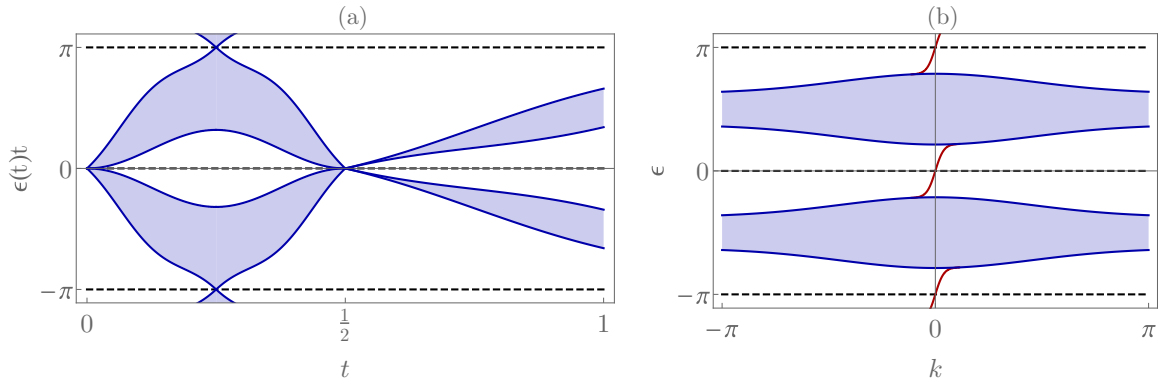

FIG. 1. (a) Unitary evolution as a composition of a loop with a constant Hamiltonian evolution. Instantaneous quasienergy bands are shown in blue. (b) End point of this unitary evolution, with quasienergy bands shown in blue and edge modes (which may be present in the open system) shown in red. The full spectrum has been projected onto a single momentum direction, labeled by k.

D. Compositions and homotopy of unitary evolutions

Before outlining the classification scheme in detail, we describe a few properties of unitary evolutions that we will require below. We will need to consider compositions of unitaries, and so, borrowing notation from the composition of paths [63], we write the evolution due to U_1 followed by the evolution due to U_2 as $U_1 * U_2$. If $H_1(\mathbf{k},t)$ is the Hamiltonian corresponding to U_1 and $H_2(\mathbf{k},t)$ is the Hamiltonian corresponding to U_2, the Hamiltonian corresponding to the composition $U_1 * U_2$ is given by

$$H(t) = \begin{cases} H_1(\mathbf{k},2t) & 0 \leqslant t \leqslant 1/2 \\ H_2(\mathbf{k},2t-1) & 1/2 \leqslant t \leqslant 1 \end{cases}. \tag{9}$$

With this definition, the endpoint of any composition of unitaries always occurs at $t = 1$.

In general, this composition rule produces an evolution that is no longer time-reversal symmetric about $t = T/2$, even if H_1 and H_2 individually *are* symmetric. The discussions below become considerably simpler if the composite Hamiltonian retains our definition of TRS. For this reason, if we wish to consider systems with TRS, we should instead define the Hamiltonian corresponding to the composition $U_1 * U_2$ by

$$H(t) = \begin{cases} H_2(\mathbf{k},2t) & 0 \leqslant t \leqslant 1/4 \\ H_1(\mathbf{k},2t-1/2) & 1/4 \leqslant t \leqslant 3/4 \\ H_2(\mathbf{k},2t-1) & 3/4 \leqslant t \leqslant 1 \end{cases}, \tag{10}$$

which we see has the required symmetry.

For classification purposes, we split the set $\mathcal{U}_g^{\mathcal{S}}$ into equivalence classes. Following the classification scheme of static topological insulators in Ref. [10], we carry out this partition using homotopy. We define homotopy in the usual way, and say that two unitary operators $U_1, U_2 \in \mathcal{U}_g^{\mathcal{S}}$ are homotopic if and only if there exists a function $h(s)$, with $s \in [0,1]$, such that

$$h(0) = U_1, \qquad h(1) = U_2, \tag{11}$$

with $h(s) \in \mathcal{U}_g^{\mathcal{S}}$ for all intermediate values of s. In this way, the gap structure at $t = 1$ (but only the gap structure at this point) must be preserved throughout the homotopy. We write homotopy equivalence as $U_1 \approx U_2$.

In order to compare unitaries with different numbers of bands, we introduce the further equivalence relation of stable homotopy as follows. We define $U_1 \sim U_2$ if and only if there exist two trivial unitaries, $U_{n_1}^0$ and $U_{n_2}^0$, such that

$$U_1 \oplus U_{n_1}^0 \approx U_2 \oplus U_{n_2}^0, \tag{12}$$

where $\oplus$ is the direct sum and n_1, n_2 are positive integers that give the number of bands in the trivial unitary. The appropriate trivial unitaries U_n^0 must belong to the set $\mathcal{U}_g^{\mathcal{S}}$, and will be given explicitly when required.

Finally, since we are ultimately interested in the behavior at a system boundary, the discussion is simplified considerably if we also define equivalence classes of pairs of unitaries. The pairs (U_1, U_2) and (U_3, U_4), where both members of each pair have the same number of bands, are stably homotopic if and only if

$$U_1 \oplus U_4 \sim U_2 \oplus U_3. \tag{13}$$

We write this equivalence as $(U_1, U_2) \sim (U_3, U_4)$.

III. DECOMPOSITION OF UNITARY EVOLUTIONS

Our approach will be to isolate the new, dynamical topological behavior from the static topological behavior that is encoded in a nontrivial Floquet Hamiltonian. We will initially restrict the discussion to unitaries that have gaps at both $\epsilon = 0$ and $\epsilon = \pi$ (with possible additional gaps elsewhere in the spectrum), considering more general cases in Sec. V. We write the set of such unitaries as $\mathcal{U}_{0,\pi}^{\mathcal{S}}$.

To proceed, it is useful to define two special types of unitary evolution. First, we define a unitary loop to be a unitary evolution that satisfies $U(\mathbf{k},0) = U(\mathbf{k},1) = \mathbb{I}$. A unitary of this form can be seen to act trivially on a closed system but may generate nontrivial edge modes in a system with a boundary. Secondly, we define a constant Hamiltonian evolution as a unitary evolution that may be expressed as $U(\mathbf{k},t) = e^{-iH(\mathbf{k})t}$ for some static Hamiltonian $H(\mathbf{k})$, whose eigenvalues have magnitude strictly less than π. The utility of identifying these two types of unitary evolutions becomes apparent when one considers the following theorem:

Theorem III.1. Every unitary $U \in \mathcal{U}^{\mathcal{S}}_{0,\pi}$ can be continuously deformed to a composition of a unitary loop L and a constant Hamiltonian evolution C, which we write as $U \approx L * C$. L and C are unique up to homotopy.

Theorem III.1 is proved in Appendix C and is illustrated schematically in Fig. 1(a). By a slight abuse of terminology, we will often call the unitary composed of the loop and the constant the 'decomposition' of the original unitary. Heuristically, the decomposition can be interpreted as an initial loop, which may generate nontrivial edge modes at $\epsilon = \pi$, followed by a constant evolution by the static Floquet Hamiltonian H_F. Since we have assumed there is a spectral gap at $\epsilon = \pi$, the branch cut required for the definition in Eq. (8) can be placed in this region, and the final quasienergy bands can be consistently thought of as emanating from the point $\epsilon = 0$. In addition, since we are assuming that the complete unitary evolution is gapped at both $\epsilon = 0$ and $\epsilon = \pi$, the static Hamiltonian required for the constant evolution must be gapped at zero. We write the set of unitary loops in symmetry class $\mathcal{S}$ as $\mathcal{U}^{\mathcal{S}}_L$ and the set of constant, gapped Floquet Hamiltonian evolutions in symmetry class $\mathcal{S}$ as $\mathcal{U}^{\mathcal{S}}_C$.

Through this unique decomposition, we see that a general unitary evolution from $\mathcal{U}_{0,\pi}$ can be classified by separately considering the unitary loop component and the constant evolution component. A specific phase may be labeled by the pair (n_L, n_C), where n_L and n_C are invariant integers associated with the unitary loop and constant evolution components, respectively.

Next, we label the set of static gapped Hamiltonians in symmetry class $\mathcal{S}$, whose eigenvalues E satisfy $0 < |E| < \pi$, by $\mathcal{H}^{\mathcal{S}}$. The set of gapped Floquet Hamiltonian evolutions in $\mathcal{U}^{\mathcal{S}}_C$ is clearly in one-to-one correspondence with the set of static Hamiltonians in $\mathcal{H}^{\mathcal{S}}$. This follows from the bijection $C(t) = \exp(-iH_F t)$, where H_F is the unique Floquet Hamiltonian with eigenvalue magnitude strictly between 0 and π. From the definition of homotopy given in Sec. II D, we see that $C_1 \approx C_2$ within $\mathcal{U}^{\mathcal{S}}_C$ if and only if $H_1 \approx H_2$ within $\mathcal{H}^{\mathcal{S}}$, where H_i is the static Hamiltonian corresponding to C_i. In addition, it follows that $C_1 \sim C_2$ if and only if $H_1 \sim H_2$, if we write the trivial unitary as

$$U^0_n(\mathbf{k},t) = \exp\big(-iH^0_n\big), \tag{14}$$

where H^0_n is a suitable trivial Hamiltonian.

In this way, we can classify pairs of constant Hamiltonian evolutions (C_1, C_2) by instead classifying pairs of static Hamiltonians (H_1, H_2). This is a relative classification that is equivalent to the well-known classification of static topological insulators, which is summarized in the periodic table given in Ref. [10]. The classification of pairs of unitary loops (L_1, L_2) does not, however, have a static analog.

Through this decomposition, the periodic table of static topological insulators may be viewed as a subset of a larger classification scheme that also includes time-dependent Hamiltonians. In this picture, static topological insulators correspond to compositions of nontrivial constant Hamiltonian evolutions with trivial unitary loops. More general dynamical topological phases arise through compositions of constant evolutions with *nontrivial* unitary loops. In the next section of this paper we set out to classify the nontrivial unitary loops that may exist in each symmetry class.

IV. CLASSIFICATION OF UNITARY LOOPS

A. Unitary loops with particle-hole symmetry only

With the machinery defined in previous sections, we are now ready to give a systematic discussion of the classification of unitary loops. We begin by considering loops in systems that have PHS but no other symmetry, belonging to the set $\mathcal{U}^{\mathcal{S}}_L$ with $\mathcal{S} \in \{\mathrm{C},\mathrm{D}\}$.

1. Hermitian maps

To proceed, we define a Hermitian map corresponding to a given unitary $U(\mathbf{k},t)$ through

$$H_U(\mathbf{k},t) = \begin{pmatrix} 0 & U(\mathbf{k},t) \\ U^\dagger(\mathbf{k},t) & 0 \end{pmatrix}, \tag{15}$$

which we see satisfies $H^2_U = \mathbb{I}$. In addition, we define the two new symmetry operations

$$P_1 = \begin{pmatrix} P & 0 \\ 0 & P \end{pmatrix}, \qquad P_2 = \begin{pmatrix} P & 0 \\ 0 & -P \end{pmatrix}, \tag{16}$$

which are derived from the standard PHS operator P. Using Eq. (4), we see that the Hermitian map satisfies the following new symmetry relations:

$$\begin{aligned} P_1 H_U(\mathbf{k},t) P_1^{-1} &= H^*_U(-\mathbf{k},t) \\ P_2 H_U(\mathbf{k},t) P_2^{-1} &= -H^*_U(-\mathbf{k},t). \end{aligned} \tag{17}$$

We write the set of Hermitian maps that square to the identity, satisfy these symmetries, and which additionally satisfy $H_U(\mathbf{k},0) = H_U(\mathbf{k},1)$ (but which are not necessarily derived from unitary loops) as $\mathscr{H}^{\mathcal{S}}$. We write the subset of $\mathscr{H}^{\mathcal{S}}$ that corresponds specifically to unitary loops as $\mathscr{H}^{\mathcal{S}}_L$, and note that from the properties of unitary loops, members of $\mathscr{H}^{\mathcal{S}}_L$ must satisfy

$$H_U(\mathbf{k},0) = H_U(\mathbf{k},1) = \begin{pmatrix} 0 & \mathbb{I}_n \\ \mathbb{I}_n & 0 \end{pmatrix}. \tag{18}$$

There is a one-to-one mapping between a unitary loop $U \in \mathcal{U}^{\mathcal{S}}_L$ and the corresponding Hermitian map $H_U \in \mathscr{H}^{\mathcal{S}}_L$, a statement that is proved in Appendix D.

It is easy to verify that $U_1 \approx U_2$ if and only if $H_{U_1} \approx H_{U_2}$, which extends the definition of homotopy equivalence to $\mathscr{H}^{\mathcal{S}}$. Next, we note that the trivial unitary loop is given by

$$U^0_n(\mathbf{k},t) = \mathbb{I}_n, \tag{19}$$

and the corresponding trivial matrix in $\mathscr{H}^{\mathcal{S}}_L$ is given by

$$H^0_{U,n}(\mathbf{k},t) = \begin{pmatrix} 0 & \mathbb{I}_n \\ \mathbb{I}_n & 0 \end{pmatrix}. \tag{20}$$

This allows us to define the stable homotopy equivalence of Hermitian maps through

$$H_A \sim H_B \;\Leftrightarrow\; H_A \oplus H^0_{U,n_1} \approx H_B \oplus H^0_{U,n_2}, \tag{21}$$

in the space $\mathscr{H}^{\mathcal{S}}_L$. Again, it is clear that $U_1 \sim U_2 \Leftrightarrow H_{U_1} \sim H_{U_2}$.

As in the case of unitaries, we can also consider pairs of Hermitian maps, (H_{U_1}, H_{U_2}), where both members of each pair have the same number of bands. This allows us to define the equivalence relation $(H_{U_1}, H_{U_2}) \sim (H_{U_3}, H_{U_4})$ if and only

if $H_{U_1} \oplus H_{U_4} \sim H_{U_3} \oplus H_{U_2}$. These pairs of Hermitian maps form an additive group, described in Appendix E, which we can use to classify the relative topological invariants of the corresponding pair of unitary evolutions.

2. Classification of unitaries using K theory

We will omit the technical steps of the K-theory argument in this section and instead give an overview of the method. For further details, we refer the reader to Appendix E and references therein.

The general idea is to use the Morita equivalence of categories to map the group of equivalence classes of pairs in $\mathscr{H}^{\mathcal{S}}$ onto a K group of the kind $KR^{0,q}(M)$ [or, later, $K(M)$ for classes A and AIII]. The $KR^{0,q}(M)$ are a set of well-studied K groups of manifolds which are described, for example, in Refs. [64–66]. In these expressions, M is the manifold $S^1 \times X$, where X is the Brillouin zone and S^1 is the circle corresponding to the time direction, whose initial and final points ($t = 0$ and $t = 1$) are identified due to the assumed periodicity of Hermitian maps in $\mathscr{H}^{\mathcal{S}}$. The space M is, in the terminology of Ref. [66], a *real space*, i.e., a space with an involution corresponding to $\mathbf{k} \to -\mathbf{k}$. The reduction using Morita equivalence relations is equivalent to Kitaev's trick of replacing negative generators with positive generators [10].

For class D, the resulting group of the equivalence classes of pairs is $KR^{0,1}(S^1 \times X)$, while for class C the resulting group is $KR^{0,5}(S^1 \times X)$. Specifically restricting ourselves to the subset $\mathscr{H}_L^{\mathcal{S}}$, the group of equivalence classes of pairs of loops is then isomorphic to the relative K group

$$\begin{aligned} KR^{0,1}(S^1 \times X, \{0\} \times X) &= KR^{0,2}(X) \quad \text{Class D} \\ KR^{0,5}(S^1 \times X, \{0\} \times X) &= KR^{0,6}(X) \quad \text{Class C}, \end{aligned} \tag{22}$$

where the point $\{0\} \in S^1$ corresponds to the initial time of the evolution. The equalities in these two equations are well-known K-theory isomorphisms [65,66]. The last results are identical to the K groups classifying static topological insulators from these classes, and we note that the K group captures both the strong and weak invariants.

B. Unitary loops with time-reversal symmetry

We now discuss the classification of unitaries that have TRS and which may also have PHS. These correspond to the symmetry classes AI and AII (TRS only), and classes BDI, CII, DIII, and CI (TRS and PHS).

Although it is possible to work with the unitary operators directly, the calculations become considerably simpler if we instead define symmetrized unitaries, $U_S(\mathbf{k},t)$, through

$$U_S(\mathbf{k},t) = \exp\left[-i \int_{\frac{1-t}{2}}^{\frac{1+t}{2}} H(\mathbf{k},t')\, \mathrm{d}t'\right]. \tag{23}$$

It is clear that there is a one-to-one correspondence between unitary operators $U(\mathbf{k},t)$ and their symmetrized forms $U_S(\mathbf{k},t)$, and further, that both expressions agree at $t = 0$ and $t = 1$. Under a particle-hole transformation, a symmetrized unitary with PHS satisfies the same relation as the original unitary,

$$PU_S(\mathbf{k},t)P^{-1} = U_S^*(-\mathbf{k},t), \tag{24}$$

while under time reversal, the symmetrized unitary operator transforms as

$$\theta U_S(\mathbf{k},t)\theta^{-1} = U_S^{\dagger *}(-\mathbf{k},t), \tag{25}$$

relations that are derived in Appendix B. For the rest of this section we will drop the subscript S and assume that we are using symmetrized unitaries.

As in the previous section, a (symmetrized) unitary evolution that belongs to $\mathcal{U}_{0,\pi}^{\mathcal{S}}$ is equivalent to a composition of a unitary loop with a constant Hamiltonian evolution. However, since the unitaries involved now have TRS, composition is defined using the time-reversal symmetric expression in Eq. (10). The classification of the constant Hamiltonian evolution component follows the discussion in Sec. III, with topological edge modes at $\epsilon = \pi$, if present, arising from the loop component.

1. Hermitian maps

To classify the unitary loops in these classes, we again define a Hermitian map corresponding to a given (symmetrized) unitary $U(\mathbf{k},t)$ as in Eq. (15). This time, we require up to four symmetry operators,

$$\begin{aligned} P_1 &= \begin{pmatrix} P & 0 \\ 0 & P \end{pmatrix}, \qquad P_2 = \begin{pmatrix} P & 0 \\ 0 & -P \end{pmatrix}, \\ \theta_1 &= \begin{pmatrix} 0 & \theta \\ \theta & 0 \end{pmatrix}, \qquad \theta_2 = \begin{pmatrix} 0 & \theta \\ -\theta & 0 \end{pmatrix}, \end{aligned} \tag{26}$$

which are derived from the symmetry operators P and θ. If the relevant symmetry is present, these operators act on the Hermitian map H_U to give

$$\begin{aligned} P_1 H_U(\mathbf{k},t) P_1^{-1} &= H_U^*(-\mathbf{k},t) \\ P_2 H_U(\mathbf{k},t) P_2^{-1} &= -H_U^*(-\mathbf{k},t) \end{aligned} \tag{27}$$

for classes BDI, CII, DIII, and CI, and

$$\begin{aligned} \theta_1 H_U(\mathbf{k},t) \theta_1^{-1} &= H_U^*(-\mathbf{k},t) \\ \theta_2 H_U(\mathbf{k},t) \theta_2^{-1} &= -H_U^*(-\mathbf{k},t) \end{aligned} \tag{28}$$

for classes AI, AII, BDI, CII, DIII, and CI.

As before, we write the set of Hermitian maps that square to the identity, satisfy these symmetries, and which additionally satisfy $H_U(\mathbf{k},0) = H_U(\mathbf{k},1)$, as $\mathscr{H}^{\mathcal{S}}$, and write the subset of this that corresponds to unitary loops as $\mathscr{H}_L^{\mathcal{S}}$. There is again a one-to-one mapping between the set of $U \in \mathcal{U}_L^{\mathcal{S}}$ and the corresponding set of Hermitian maps $H_U \in \mathscr{H}_L^{\mathcal{S}}$, a statement that can be proved using a method similar to that given in Appendix D. As in Sec. IV A, homotopy, stable homotopy, and the equivalence of pairs can be defined for Hermitian maps in $\mathscr{H}^{\mathcal{S}}$.

2. Classification of unitaries using K theory

We can now use K-theory arguments to map the equivalence classes of pairs in $\mathscr{H}^{\mathcal{S}}$ onto K groups. Using the arguments of Sec. IV A for each symmetry class, we find the group of

equivalence classes in each case maps onto

$$\begin{array}{ll} KR^{0,7}(S^1\times X) & \text{Class AI} \\ KR^{0,3}(S^1\times X) & \text{Class AII} \\ KR^{0,0}(S^1\times X) & \text{Class BDI} \\ KR^{0,4}(S^1\times X) & \text{Class CII} \\ KR^{0,2}(S^1\times X) & \text{Class DIII} \\ KR^{0,6}(S^1\times X) & \text{Class CI.} \end{array} \tag{29}$$

Restricting to the subset $\mathscr{H}_L^{\mathcal{S}}$, the groups are then isomorphic to the relative K groups

$$\begin{aligned} KR^{0,7}(S^1\times X,\{0\}\times X) &= KR^{0,0}(X) && \text{Class AI} \\ KR^{0,3}(S^1\times X,\{0\}\times X) &= KR^{0,4}(X) && \text{Class AII} \\ KR^{0,0}(S^1\times X,\{0\}\times X) &= KR^{0,1}(X) && \text{Class BDI} \\ KR^{0,4}(S^1\times X,\{0\}\times X) &= KR^{0,5}(X) && \text{Class CII} \\ KR^{0,2}(S^1\times X,\{0\}\times X) &= KR^{0,3}(X) && \text{Class DIII} \\ KR^{0,6}(S^1\times X,\{0\}\times X) &= KR^{0,7}(X) && \text{Class CI,} \end{aligned} \tag{30}$$

using a set of well-known K-theory isomorphisms as outlined in Appendix E [65,66]. The last results are identical to the K groups classifying static topological insulators from these classes and describe the complete set of strong and weak invariants. Overall, it follows that pairs of unitary loops within $\mathcal{U}_L^{\mathcal{S}}$ are classified by the K groups given in Eq. (30).

C. Classification of gapped unitaries in symmetry classes A and AIII

Finally, we discuss the classification of time evolution unitaries in the complex symmetry classes, with $\mathcal{S}\in\{\text{A},\text{AIII}\}$. As in the previous section, the discussion is simplified if we use the symmetrized unitaries $U_S(\mathbf{k},t)$ defined in Eq. (23). In terms of these, the chiral symmetry operator (relevant for class AIII) has the action

$$CU_S(\mathbf{k},t)C^{-1}=U_S^\dagger(\mathbf{k},t), \tag{31}$$

a relation that is derived in Appendix B. As before, we will drop the subscript S and assume we are working with symmetrized unitaries throughout this section.

1. Hermitian maps

As in the previous cases, we use Eq. (15) to define a Hermitian map $H_U(\mathbf{k},t)$ (satisfying $H_U^2=\mathbb{I}$), which corresponds to a given (symmetrized) unitary $U(\mathbf{k},t)$. The relevant symmetry operators for classes A and AIII are

$$\Sigma=\begin{pmatrix}\mathbb{I} & 0\\ 0 & -\mathbb{I}\end{pmatrix},\qquad \Gamma=\begin{pmatrix}0 & C\\ -C & 0\end{pmatrix}. \tag{32}$$

The first of these anticommutes with any Hermitian map of the form H_U, while the second, which is derived from the CS operator C, is relevant only for class AIII. These operators act on H_U to give

$$\begin{aligned} \Sigma H_U(\mathbf{k},t)\Sigma^{-1} &= -H_U(\mathbf{k},t) && \text{Classes A and AIII} \\ \Gamma H_U(\mathbf{k},t)\Gamma^{-1} &= -H_U(\mathbf{k},t) && \text{Class AIII.} \end{aligned} \tag{33}$$

We write the set of Hermitian maps that square to the identity, satisfy these symmetries, and which additionally satisfy $H_U(\mathbf{k},0)=H_U(\mathbf{k},1)$ as $\mathscr{H}^{\mathcal{S}}$, and write the subset of this that corresponds to unitary loops as $\mathscr{H}_L^{\mathcal{S}}$. There is again a one-to-one mapping between the set of $U\in\mathcal{U}_L^{\mathcal{S}}$ and the corresponding set of Hermitian maps $H_U\in\mathscr{H}_L^{\mathcal{S}}$, a statement that can be proved using the method of Appendix D. Homotopy, stable homotopy, and equivalence of pairs in $\mathscr{H}^{\mathcal{S}}$ can be defined as in previous sections.

2. Classification of unitaries using K theory

We can now use K-theory arguments to map the equivalence classes of pairs in $\mathscr{H}^{\mathcal{S}}$ onto K groups. For each symmetry class, we find the mapping to

$$\begin{array}{ll} K^1(S^1\times X) & \text{Class A} \\ K^2(S^1\times X) & \text{Class AIII.} \end{array} \tag{34}$$

Restricting to the subset $\mathscr{H}_L^{\mathcal{S}}$, the groups are then isomorphic to the relative K groups

$$\begin{aligned} K^1(S^1\times X,\{0\}\times X) &= K^0(X) && \text{Class A} \\ K^2(S^1\times X,\{0\}\times X) &= K^1(X) && \text{Class AIII,} \end{aligned} \tag{35}$$

which follow from known K-theory isomorphisms [65,66]. The last results are identical to the K groups classifying static topological insulators from these classes, and it follows overall that pairs of unitary loops from classes A and AIII are classified by the K groups given in Eq. (35). The K groups capture the complete set of strong and weak invariants.

V. DISCUSSION

A. Complete classification of unitary evolutions

In the preceding section we obtained groups for the equivalence classes of pairs of unitary loops from the ten AZ symmetry classes. These groups are of the form $KR^{0,q}(X)$ for real symmetry classes and of the form $K^q(X)$ for complex symmetry classes, where X is the Brillouin zone torus. The final K groups were given in Eqs. (22), (30), and (35).

We noted that these K groups are identical to those obtained from the topological classification of static (single-gapped) Hamiltonians in the same symmetry classes. Depending on the dimension of the Brillouin zone X, these K groups are isomorphic to a group $\mathcal{G}\in\{\emptyset,\mathbb{Z}_2,\mathbb{Z}\}$, reproducing the well-known periodic table of topological insulators and superconductors [10].

A general unitary evolution, however, will not correspond directly to a loop evolution. As discussed in Sec. III, we can decompose a unitary evolution that is gapped at both $\epsilon=0$ and $\epsilon=\pi$ into a loop followed by an evolution with a static Hamiltonian. More generally, there may be gaps present in the endpoint spectrum at other quasienergies. In this way, to completely classify the space of gapped unitary evolutions, we must first identify the different end point gap structures that are compatible with each symmetry class.

1. Systems without particle-hole or chiral symmetry

In systems without PHS or CS (classes A, AI, and AII), there are no restrictions on the quasienergies at which physically relevant gaps may occur. To see this, we can imagine composing a unitary evolution U, which has a gap at ϵ_0, with an evolution by a trivial Hamiltonian proportional to the identity, $U_0=e^{-it\mathbb{I}}$. For class A, the evolution by U_0 can simply follow the

TABLE II. Classification of gapped unitary evolutions by symmetry class and spatial dimension d. The number of relevant spectral gaps is given by $n_p \in \{1,2\}$ for systems with PHS or CS and by $n \in \mathbb{Z}^+$ for systems without PHS or CS. The table repeats for $d \geqslant 8$ (Bott periodicity).

$\mathcal{S}$	$d=0$	1	2	3	4	5	6	7
A	$\mathbb{Z}^{\times n}$	$\emptyset$	$\mathbb{Z}^{\times n}$	$\emptyset$	$\mathbb{Z}^{\times n}$	$\emptyset$	$\mathbb{Z}^{\times n}$	$\emptyset$
AIII	$\emptyset$	$\mathbb{Z}^{\times n_p}$	$\emptyset$	$\mathbb{Z}^{\times n_p}$	$\emptyset$	$\mathbb{Z}^{\times n_p}$	$\emptyset$	$\mathbb{Z}^{\times n_p}$
AI	$\mathbb{Z}^{\times n}$	$\emptyset$	$\emptyset$	$\emptyset$	$\mathbb{Z}^{\times n}$	$\emptyset$	$\mathbb{Z}_2^{\times n}$	$\mathbb{Z}_2^{\times n}$
BDI	$\mathbb{Z}_2^{\times n_p}$	$\mathbb{Z}^{\times n_p}$	$\emptyset$	$\emptyset$	$\emptyset$	$\mathbb{Z}^{\times n_p}$	$\emptyset$	$\mathbb{Z}_2^{\times n_p}$
D	$\mathbb{Z}_2^{\times n_p}$	$\mathbb{Z}_2^{\times n_p}$	$\mathbb{Z}^{\times n_p}$	$\emptyset$	$\emptyset$	$\emptyset$	$\mathbb{Z}^{\times n_p}$	$\emptyset$
DIII	$\emptyset$	$\mathbb{Z}_2^{\times n_p}$	$\mathbb{Z}_2^{\times n_p}$	$\mathbb{Z}^{\times n_p}$	$\emptyset$	$\emptyset$	$\emptyset$	$\mathbb{Z}^{\times n_p}$
AII	$\mathbb{Z}^{\times n}$	$\emptyset$	$\mathbb{Z}_2^{\times n}$	$\mathbb{Z}_2^{\times n}$	$\mathbb{Z}^{\times n}$	$\emptyset$	$\emptyset$	$\emptyset$
CII	$\emptyset$	$\mathbb{Z}^{\times n_p}$	$\emptyset$	$\mathbb{Z}_2^{\times n_p}$	$\mathbb{Z}_2^{\times n_p}$	$\mathbb{Z}^{\times n_p}$	$\emptyset$	$\emptyset$
C	$\emptyset$	$\emptyset$	$\mathbb{Z}^{\times n_p}$	$\emptyset$	$\mathbb{Z}_2^{\times n_p}$	$\mathbb{Z}_2^{\times n_p}$	$\mathbb{Z}^{\times n_p}$	$\emptyset$
CI	$\emptyset$	$\emptyset$	$\emptyset$	$\mathbb{Z}^{\times n_p}$	$\emptyset$	$\mathbb{Z}_2^{\times n_p}$	$\mathbb{Z}_2^{\times n_p}$	$\mathbb{Z}^{\times n_p}$

evolution U, while for classes AI and AII, the TR-symmetric composition given in Eq. (10) should be used. The composition $U * U_0$ therefore remains within the specified symmetry class but continuously moves the quasienergy gap at ϵ_0 to $\epsilon_0 + t$ (modulo 2π). Any edge modes initially present at ϵ_0 will be moved with the gap. In these symmetry classes, there is nothing special about the gaps at $\epsilon = 0$ and $\epsilon = \pi$, even though we implicitly assumed gaps at these points in the main text.

Therefore, if there is only one gap present in the end point spectrum, we can always (temporarily) shift it to $\epsilon = \pi$, continuously and while preserving the symmetry. The resulting unitary can then be deformed to a loop, and follows the K-theory classification outlined in Sec. IV. In this way, a single-gapped unitary evolution without PHS or CS is classified by the group $\mathcal{G} \in \{\emptyset, \mathbb{Z}_2, \mathbb{Z}\}$, depending on the AZ symmetry class.

If there are several gaps in the end point spectrum, we can continuously rotate it so that one gap arises at $\epsilon = \pi$. Then, following the arguments of Sec. III, the unitary evolution may be decomposed into a loop followed by a constant Hamiltonian evolution. The loop piece is classified by the K group $KR^{0,q}(X)$ or $K^q(X)$, and the constant piece is one-to-one correspondence with a static Hamiltonian. The gaps of the static Hamiltonian are classified by the same K groups $KR^{0,q}(X)$ or $K^q(X)$ as the unitary loop, and so the complete classification contains a factor of $\mathcal{G}$ for each gap in the quasienergy spectrum. An alternative way to see this is to imagine rotating each gap in the spectrum to $\epsilon = \pi$ in turn. Then, using the classification of unitary loops, we see that each gap contributes a factor of $\mathcal{G}$.

Overall, a gapped unitary evolution without PHS or CS may have $n \in \mathbb{Z}^+$ physically relevant gaps at its end point. The topological classification of such a system is given by $\mathcal{G}^{\times n}$, where $\mathcal{G} \in \{\emptyset, \mathbb{Z}_2, \mathbb{Z}\}$ depends on the AZ symmetry class and is given in Table II.

2. *Systems with particle-hole or chiral symmetry*

In systems with particle-hole symmetry (classes BDI, D, DIII, CII, C, CI) or chiral symmetry (class AIII), the quasienergies $\epsilon = 0$ and $\epsilon = \pi$ are special: It is about these points that the spectrum has the full symmetry of the system, and eigenstates at these points have symmetry-related partners at the same quasienergy. In an open system, any topologically protected edge modes will appear at one of these gaps.

In this way, for a unitary evolution with PHS or CS, physically relevant spectral gaps may occur at one or both of $\epsilon = 0$ and $\epsilon = \pi$. If only the gap at $\epsilon = \pi$ is present, then the evolution may be homotopically deformed to a loop without closing the gap. The classification of such an evolution is then given by the corresponding K group derived in Sec. IV. If gaps at both $\epsilon = \pi$ and $\epsilon = 0$ are present, then the evolution may be continuously deformed to a loop followed by a constant Hamiltonian evolution. The loop part of the evolution may be classified as before and, as argued in Sec. III, the constant evolution is in one-to-one correspondence with a static Hamiltonian, and follows the usual classification scheme for static topological insulators. The complete classification therefore has an additional factor of $KR^{0,q}(X)$ (for real symmetry classes) or $K^q(X)$ (for complex symmetry classes), corresponding to the constant part of the evolution. Overall, a unitary evolution with gaps at both $\epsilon = 0$ and $\epsilon = \pi$ has the classification $\mathcal{G} \times \mathcal{G} \in \{\emptyset, \mathbb{Z}_2 \times \mathbb{Z}_2, \mathbb{Z} \times \mathbb{Z}\}$, depending on the specific K group.

Finally, we consider the case where there is only a gap at $\epsilon = 0$. Since there is no gap at $\epsilon = \pi$, we cannot continuously deform the unitary evolution into a loop followed by a constant Hamiltonian evolution (recall that we require the constant Hamiltonian to have instantaneous eigenvalues strictly between $-\pi$ and π). In contrast to the cases without PHS or CS considered in Sec. V A 1, we also cannot rotate the spectrum by composing the unitary with a trivial evolution, as this composition would not preserve the symmetry. There is, however, a *mapping* between the endpoint unitary with a gap at $\epsilon = 0$ and the end point unitary that has been rotated by $\Delta\epsilon = \pi$ so that the gap is now at $\epsilon = \pi$.

For instance, in the simplest case of class AIII, we may choose the symmetry operator to take the form $C = \sigma_3 \otimes \mathbb{I}$, which acts as σ_3 on the two sublattices on each site. Then, the map produced by evolving with the Hamiltonian $H = \pi\sigma_1 \otimes \mathbb{I}$ has the final form $e^{iH} = -1$, which changes the eigenvalues of the previous eigenstates but not their spatial dependence. The final unitary $U = -1$ therefore maps all edge state at $\epsilon = 0$ onto edge states at $\epsilon = \pi$. Thus, from our previous K theory classification, we conclude that unitaries with a gap at $\epsilon = 0$ have the same classification as unitaries with a gap at $\epsilon = \pi$, and so also have the same edge behavior. A similar technique may be used for all other symmetry classes with PHS or CS. In this way, the classification of unitary evolutions with a single gap at $\epsilon = 0$ is also given by $\mathcal{G} \in \{\emptyset, \mathbb{Z}_2, \mathbb{Z}\}$, depending on the specific K group.

Overall, we see that a gapped unitary evolution with PHS or CS may have $n_p \in \{1,2\}$ physically relevant gaps at its end point. The topological classification of such a system is given by $\mathcal{G}^{\times n_p}$, where $\mathcal{G} \in \{\emptyset, \mathbb{Z}_2, \mathbb{Z}\}$ depends on the AZ symmetry class.

The classification of noninteracting gapped unitary evolutions is summarized in the periodic table given in Table II, with entries listed according to symmetry class, dimension,

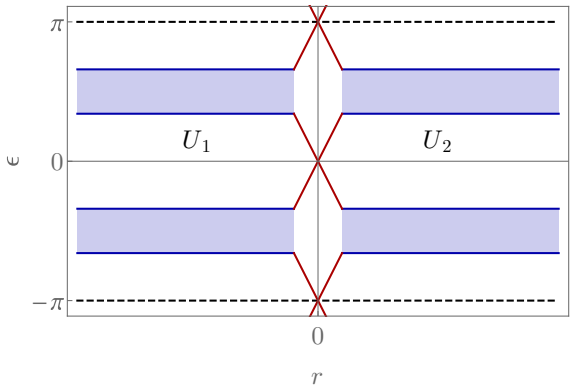

FIG. 2. Schematic diagram of the interface between a system described by unitary U_1 and a system described by unitary $U_2 \neq U_1$. The vertical axis shows the quasienergy spectrum at $t = T$ and the horizontal axis gives the displacement, with the interface occurring in the neighborhood around $r = 0$. Bulk bands are shown in blue, with protected edge modes shown in red at the interface.

and endpoint gap structure. It may be noted that the periodic table for static topological insulators is contained within this dynamical periodic table: Static topological insulators correspond to evolutions with a trivial unitary loop component, which, in our generalized classification scheme, leads to one factor of the classifying group $\mathcal{G}^{\times n_P}$ or $\mathcal{G}^{\times n}$ being trivial.

B. Bulk-edge correspondence

At the interface between a system described by unitary U_1 and a system described by unitary U_2, the principle of bulk-edge correspondence asserts that there should exist protected edge modes, shown schematically in Fig. 2. A particular edge mode can be labeled by a quantum number, and the complete set of quantum numbers is isomorphic to the set of equivalence classes of (U_1, U_2). We can therefore determine the quantum number of the edge modes by appealing to the bulk classification scheme given above.

We first consider systems without PHS or CS, which may have any number of gaps n. As discussed in Sec. V A, in these cases we can always rotate the final spectrum so that one gap arises at $\epsilon = \pi$. Then, the classification described above gives one integer n_L corresponding to the loop component, and $(n-1)$ integers n_{C_i} corresponding each other gap, which derive from the gap classification of the corresponding static Hamiltonian. We write the quantum numbers associated with the edge modes as n_π for the gap at $\epsilon = \pi$ and n_i for the edge modes in each other (ith) gap.

We leave a full discussion of the bulk-edge correspondence to future work, but for completeness, we note here that the two sets of integers are related through

$$\begin{aligned} n_\pi &= n_L \\ n_i &= n_{C_i} + n_L, \end{aligned} \tag{36}$$

where addition is again taken modulo two for systems with a $\mathbb{Z}_2$ classification. In general, we see that the edge modes associated with each gap may be different.

Alternatively, as described in Sec. V A 1, we can also classify the gaps of a system without PHS or CS by rotating the spectrum so that each gap occurs at $\epsilon = \pi$ in turn and then calculating the corresponding loop invariants. This gives a loop invariant n_{L_i} for each gap in the spectrum, which maps directly onto the corresponding number of edge modes n_i.

We now consider unitary evolutions with PHS or CS, which may have gaps at one or both of $\epsilon = 0$ and $\epsilon = \pi$. If there is just one gap, the bulk index described above maps directly onto the number edge modes. In the more interesting case, there may be gaps and edge modes at both $\epsilon = 0$ and $\epsilon = \pi$. A unitary evolution of this form is classified in the bulk by a pair of integers from the appropriate group $\mathcal{G} \times \mathcal{G}$, according to Table II. We write the integer associated with the loop component as n_L and the integer associated with the gap in the constant Hamiltonian evolution as n_C. These must have a one-to-one relation with the quantum numbers associated with the edge modes in the gaps, which we write as n_0 for the gap at $\epsilon = 0$, and as n_π for the gap at $\epsilon = \pi$.

As in the previous case, the number of edge modes in each gap is related to the bulk invariants through

$$\begin{aligned} n_\pi &= n_L \\ n_0 &= n_C + n_L, \end{aligned} \tag{37}$$

where addition is taken modulo two for systems with a $\mathbb{Z}_2$ classification.

C. Strong and weak topological invariants

A number of explicit dynamical topological invariants have been proposed for various symmetry classes [34,36,38,39,41]. Our aim here is not to provide an exhaustive list of these expressions, but we note that our mapping of unitaries onto Hamiltonians in principle allows the existing structure of topological invariants for static Hamiltonians to be applied to these dynamical systems. In many of these cases, the dynamical topological invariants can be related directly to the band invariants of the static effective Hamiltonian (see, for example, Refs. [34,39,41]).

We may also use standard K theory results relating, for instance, the K group of a torus to the K groups of spheres to infer the existence of a set of weak topological invariants, similar to those of static topological insulators and superconductors. For example, in the case of class A for $d = 3$, there is no strong invariant classifying unitary loops, just as there is no strong invariant for static Hamiltonians in class A [10]. There is, however, a set of three weak invariants associated with $2d$ cross sections of the Brillouin zone torus. Similar weak invariants exist for all other symmetry classes. For the classes which involve antiunitary symmetries, the number of invariants may be inferred using standard formulas of the type

$$\tilde{K}_{\mathbb{R}}^{d-q}(\mathbb{T}^d) \cong \bigoplus_{s=0}^{d-1} \binom{d}{r} \pi_0(R_{q-s}), \tag{38}$$

where we have used the notation of Ref. [10] for these K groups.

D. Disordered unitary evolutions

Up to this point we have considered unitary evolutions in systems with lattice translational symmetry that are protected by gaps in the quasienergy spectrum. One might worry that these evolutions are sensitive to perturbations and that a small amount of disorder could cause the gaps of the final unitary to collapse. While our analysis so far has allowed us to make rigorous statements about systems with translational symmetry, it is not directly applicable to such disordered systems. Nevertheless, as we now argue, we expect the translationally invariant systems considered previously to be representative of a set of broader Floquet phases which are robust against small local perturbations.

To argue this, we appeal to the intuition established for disordered *static* topological insulators [1,2]. In these systems, adding a moderate amount of (symmetry-respecting) disorder can localize states in the bulk without affecting the anomalous states at the edge. Topological edge modes may nevertheless exist in a mobility gap, i.e., a region in the spectrum where there are no extended states that connect different edges. Edge states may only be created or destroyed if the disordered Hamiltonian is tuned through a critical point, at which point the mobility gap collapses. As long as a mobility gap is maintained at the energy of the edge modes, the edge modes themselves are protected. In this way, the original TI classification scheme obtained for translationally invariant systems may be extended to describe a much broader set of phases. Correspondingly, the group $\mathcal{G}$ obtained using K theory continues to describe the disordered phase.

We now consider the effect of disorder on a Floquet system. The discussion differs from the static case in two main ways: First, the disorder is now time dependent, and we assume, without loss of generality, that it may be incorporated by adding a term $\lambda V_{\text{dis}}(t)$ to the translationally invariant Hamiltonian. Secondly, there may now be dynamical edge modes present in the quasienergy gap at $\epsilon = \pi$.

We can simplify the discussion using the Trotterization procedure of Refs. [56,67]. There, it was shown that a unitary evolution of the form

$$U(1) = \mathcal{T} \int_0^1 [H(t') + \lambda V(t')]\mathrm{d}t, \tag{39}$$

with $V(t)$ a small local perturbation, is equivalent to the unitary evolution

$$U(1) = \left[\mathcal{T} \int_0^1 [\lambda \tilde{V}(t')]\mathrm{d}t\right]\left[\mathcal{T} \int_0^1 [H(t')]\mathrm{d}t\right], \tag{40}$$

where $\tilde{V}(t)$ is another local perturbation related to $V(t)$ through conjugation with the unperturbed Hamiltonian. In this way, a concurrent perturbation can be 'pulled out' to the end of the evolution.

Using this procedure, we see that a weakly disordered loop is equivalent to an unperturbed loop followed by a weak disordering potential. The unperturbed loop may exhibit nontrivial loop order, which is manifested as edge modes in the gap at $\epsilon = \pi$. As long as the instantaneous unitary operator $U(t)$ (for the full system) has a mobility gap at $\epsilon = \pi$ at all times after the loop, one expects the edge modes to persist and the order to be protected.

In the more general case, the unperturbed evolution does not describe a pure loop and instead may be decomposed into a loop evolution followed by a constant Hamiltonian evolution (as described in Sec. III). This unperturbed evolution will in general have (symmetry-protected) topological order (SPT order) associated with both the loop and constant components, and may have edge modes at any of the n_p or n gaps in the quasienergy spectrum, as discussed in Sec. V B. When we follow this evolution with the disordering perturbation $\lambda \tilde{V}(t)$, the edge modes will persist as long as the unitary operator at times following the unperturbed evolution has a mobility gap at each of the edge mode quasienergies, and the SPT order will be protected.

In this way, given an arbitrary translationally invariant evolution described by $H(t)$, which leads to a gapped H_F that may exhibit edge modes, there is a set of disordered perturbations $\lambda V(t)$ (which need not be small) that allow these edge modes to persist. There is therefore a well-defined notion of SPT order for a broad range of disordered Floquet systems, and the classification introduced in this work describes well-defined Floquet topological noninteracting *phases*. Moreover, it is likely that there are strongly disordered versions of these Floquet phases (so-called called Anderson Floquet phases) which again have a set of robust edge modes. The robustness of topological Floquet systems to disorder has already been demonstrated, e.g., in the two-dimensional Class A system discussed in Ref. [37]. Further investigation of these disordered Floquet systems is an important open avenue for future research.

Finally, we note that in any realistic Floquet system there will inevitably be interactions between particles, although the strength of these interactions can often be made extremely small. Despite this, it is known that driving a system with even weak interactions can lead to heating to infinite temperature at long times [68–70]. To describe true Floquet phases, therefore, the systems we have discussed should also be stable to heating of this kind. This may likely be achieved by adding disorder to the system: In the presence of strong disorder and interactions, a system may undergo many-body localization (MBL) and avoid heating at infinite time [71–76] (see Ref. [77] for a review of MBL). The existence of MBL in dimensions higher than one is currently a matter of debate [78,79]. However, even if MBL ultimately fails at infinite times, the localization properties are believed to hold over prethermal time scales that are parametrically large. In this way, we expect the systems described in this work to be representative of true (or at least prethermal) Floquet topological phases, robust to weak interactions, in the presence of disorder.

VI. CONCLUSIONS

In this paper we have used methods from K theory to systematically classify noninteracting Floquet topological insulators across all AZ symmetry classes and dimensions. In the process, we discovered a number of new topological Floquet phases. Although the use of K theory requires the underlying systems to be translationally invariant, we have argued that the classification describes a broad set of Floquet phases that are robust to disorder. It would be interesting to see if these can be realized in an experimental setting.

Our results, summarized in Table II, show that the classification of a static topological system described by the group $\mathcal{G}$ is extended to the product group $\mathcal{G}^{\times n}$ or $\mathcal{G}^{\times n_p}$ in the time-dependent case, for a quasienergy spectrum with n_p or n gaps. Our approach uses the fact that a general time-evolution operator can be continuously deformed into a unitary loop followed by a constant Hamiltonian evolution, and the factors of $\mathcal{G}$ in the resulting classification scheme can be interpreted as arising from these two unitary components. In Sec. V we stated how this bulk classification scheme relates to the number of protected edge modes that may arise in a system with a boundary. The discussion of topological invariants and the bulk-boundary correspondence for more general band structures are interesting avenues for future work.

As noted in the introduction, some elements of our periodic table have appeared elsewhere in the literature in the context of Floquet systems, using different methods [33–36,38,39,41]. While our results are consistent with these works, a detailed comparison yields a number of differences. First, our definition of chiral symmetry differs from that of Ref. [36], and it would be worth investigating under what circumstances these definitions are equivalent and to what extent this affects the classification scheme. Secondly, Ref. [34] introduces a frequency domain formulation for the study of Floquet systems that explicitly makes use of time periodicity. It would be of interest to explore whether some variant of this approach applies to the more general unitary evolutions we have considered here.

In this noninteracting setting, the unique decomposition of a unitary evolution into two components (as defined in the text) could be proved rigorously, allowing us to separate the dynamical topological behavior from the static topological behavior of the Floquet Hamiltonian. It is likely that this unitary decomposition is applicable more generally, including in interacting systems if many-body complications are dealt with appropriately. Indeed, we use this unitary decomposition as a working assumption in Ref. [54], where it aids in the classification of Floquet SPTs in one dimension. This approach may be useful in the classification of driven, interacting topological phases more generally, a field in which much progress has recently been made [51–58].

ACKNOWLEDGMENTS

The authors would like to thank S. L. Sondhi for bringing this problem to our attention and sharing some particularly useful insights. The authors also thank D. Reiss, C. W. von Keyserlingk, B. Fregoso, and F. Zhang for fruitful discussions, thank J. Asbóth for providing useful comments on the manuscript, and thank Michael Kolodrubetz for pointing out an error in an earlier version. R.R. and F.H. acknowledge support from the NSF under CAREER DMR-1455368 and the Alfred P. Sloan foundation.

APPENDIX A: ACTION OF SYMMETRY OPERATORS ON UNITARIES

In this Appendix, we prove the action of the three symmetry operators on the time-evolution unitary. In order to simplify certain steps of the calculation, we will make use of the two-point (nonsymmetrized) unitary operators defined through

$$U(\mathbf{k};t_2,t_1) = \mathcal{T}\exp\left(-i\int_{t_1}^{t_2} H(\mathbf{k},t')\mathrm{d}t'\right), \tag{A1}$$

where we see that $U(\mathbf{k};t,0) \equiv U(\mathbf{k},t)$. These auxiliary unitaries satisfy the properties

$$\begin{aligned}[U(\mathbf{k};t_2,t_1)]^\dagger &= U(\mathbf{k};t_1,t_2)\\ U(\mathbf{k};t_3,t_1) &= U(\mathbf{k};t_3,t_2)U(\mathbf{k};t_2,t_1).\end{aligned} \tag{A2}$$

1. Particle-hole symmetry

For the PHS operator, we start from

$$PH(\mathbf{k},t)P^{-1} = -H^*(-\mathbf{k},t) \tag{A3}$$

and find

$$\begin{aligned}PU(\mathbf{k},t)P^{-1} &= P\left[\mathcal{T}\exp\left(-i\int_0^t H(\mathbf{k},t')\mathrm{d}t'\right)\right]P^{-1} = \left[\sum_n \frac{(-i)^n}{n!}\mathcal{T}\int_0^t \mathrm{d}t_1\ldots\int_0^t \mathrm{d}t_n\, PH(\mathbf{k},t_1)P^{-1}\ldots PH(\mathbf{k},t_n)P^{-1}\right]\\ &= \left[\sum_n \frac{(+i)^n}{n!}\mathcal{T}\int_0^t \mathrm{d}t_1\ldots\int_0^t \mathrm{d}t_n\, H^*(-\mathbf{k},t_1)\ldots H^*(-\mathbf{k},t_n)\right] = \left[\mathcal{T}\exp\left(-i\int_0^t H(-\mathbf{k},t')\mathrm{d}t'\right)\right]^* = U^*(-\mathbf{k},t).\end{aligned} \tag{A4}$$

2. Time-reversal symmetry

For the TRS operator, we start from

$$\theta H(\mathbf{k},t)\theta^{-1} = H^*(-\mathbf{k},T-t) \tag{A5}$$

and find

$$\begin{aligned}\theta U(\mathbf{k},t)\theta^{-1} &= \theta\left[\mathcal{T}\exp\left(-i\int_0^t H(\mathbf{k},t')\mathrm{d}t'\right)\right]\theta^{-1} = \left[\sum_n \frac{(-i)^n}{n!}\mathcal{T}\int_0^t \mathrm{d}t_1\ldots\int_0^t \mathrm{d}t_n\,\theta H(\mathbf{k},t_1)\theta^{-1}\ldots\theta H(\mathbf{k},t_n)\theta^{-1}\right]\\ &= \left[\sum_n \frac{(-i)^n}{n!}\mathcal{T}\int_0^t \mathrm{d}t_1\ldots\int_0^t \mathrm{d}t_n\,H^*(-\mathbf{k},T-t_1)\ldots H^*(-\mathbf{k},T-t_n)\right]\\ &\underset{t_i\to T-t_i}{=} \left[\sum_n \frac{(+i)^n}{n!}\mathcal{T}\int_T^{T-t} \mathrm{d}t_1\ldots\int_T^{T-t} \mathrm{d}t_n\,H^*(-\mathbf{k},t_1)\ldots H^*(-\mathbf{k},t_n)\right] = \left[\mathcal{T}\exp\left(-i\int_T^{T-t} H(-\mathbf{k},t')\mathrm{d}t'\right)\right]^*\\ &= U^*(-\mathbf{k};T-t,T). \end{aligned} \tag{A6}$$

We rewrite this using Eq. (A2) to obtain

$$\theta U(\mathbf{k},t)\theta^{-1} = U^*(-\mathbf{k};T-t,0)U^*(-\mathbf{k};0,T) = U^*(-\mathbf{k},T-t)U^{\dagger *}(-\mathbf{k},T). \tag{A7}$$

3. Chiral symmetry

For the CS operator, we start from

$$CH(\mathbf{k},t)C^{-1} = -H(\mathbf{k},T-t) \tag{A8}$$

and find

$$\begin{aligned}CU(\mathbf{k},t)C^{-1} &= C\left[\mathcal{T}\exp\left(-i\int_0^t H(\mathbf{k},t')\mathrm{d}t'\right)\right]C^{-1}\\ &= \left[\sum_n \frac{(-i)^n}{n!}\mathcal{T}\int_0^t \mathrm{d}t_1\ldots\int_0^t \mathrm{d}t_n\,CH(\mathbf{k},t_1)C^{-1}\ldots CH(\mathbf{k},t_n)C^{-1}\right]\\ &= \left[\sum_n \frac{(+i)^n}{n!}\mathcal{T}\int_0^t \mathrm{d}t_1\ldots\int_0^t \mathrm{d}t_n\,H(\mathbf{k},T-t_1)\ldots H(\mathbf{k},T-t_n)\right]\\ &\underset{t_i\to T-t_i}{=} \left[\sum_n \frac{(-i)^n}{n!}\mathcal{T}\int_T^{T-t} \mathrm{d}t_1\ldots\int_T^{T-t} \mathrm{d}t_n\,H(\mathbf{k},t_1)\ldots H(\mathbf{k},t_n)\right] = \left[\mathcal{T}\exp\left(-i\int_T^{T-t} H(\mathbf{k},t')\mathrm{d}t'\right)\right]\\ &= U(\mathbf{k};T-t,T). \end{aligned} \tag{A9}$$

We rewrite this using Eq. (A2) to obtain

$$CU(\mathbf{k},t)C^{-1} = U(\mathbf{k};T-t,0)U(\mathbf{k};0,T) = U(\mathbf{k},T-t)U^{\dagger}(\mathbf{k},T). \tag{A10}$$

APPENDIX B: ACTION OF SYMMETRY OPERATORS ON SYMMETRIZED UNITARIES

In this Appendix, we prove the action of the three symmetry operators on the symmetrized time-evolution unitaries $U_S(\mathbf{k},t)$ that are defined in Eq. (23). We will derive these relations using the corresponding expressions for the original unitaries, which we derived previously in Appendix A, and will also make use of the two-point unitaries defined in Eq. (A1). In particular, we note that

$$\begin{aligned}U_S(\mathbf{k},t) &= U\left(\mathbf{k};\frac{1+t}{2},\frac{1-t}{2}\right)\\ &= U\left(\mathbf{k};\frac{1+t}{2},0\right)U\left(\mathbf{k};0,\frac{1-t}{2}\right)\\ &= U\left(\mathbf{k},\frac{1+t}{2}\right)\left[U\left(\mathbf{k},\frac{1-t}{2}\right)\right]^{\dagger}. \end{aligned} \tag{B1}$$

We will also make use of the symmetrized unitary relation $U_S^{\dagger}(\mathbf{k},t) = U_S(\mathbf{k},-t)$.

1. Particle-hole symmetry

Starting from the unitary PHS relation

$$PU(\mathbf{k},t)P^{-1} = U^*(-\mathbf{k},t), \tag{B2}$$

we find that the symmetrized unitaries satisfy

$$\begin{aligned}PU_S(\mathbf{k},t)P^{-1} &= PU\left(\mathbf{k};\frac{1+t}{2}\right)P^{-1}P\left[U\left(\mathbf{k};\frac{1-t}{2}\right)\right]^{\dagger}P^{-1}\\ &= U^*\left(-\mathbf{k},\frac{1+t}{2}\right)\left[P^{-1}U\left(\mathbf{k},\frac{1-t}{2}\right)P\right]^{\dagger}\\ &= U^*\left(-\mathbf{k},\frac{1+t}{2}\right)\left[U^*\left(-\mathbf{k},\frac{1-t}{2}\right)\right]^{\dagger}\\ &= U_S^*(-\mathbf{k},t). \end{aligned} \tag{B3}$$

2. Time-reversal symmetry

Starting from the unitary TRS relation

$$\theta U(\mathbf{k},t)\theta^{-1} = U^*(-\mathbf{k},1-t)U^{\dagger *}(-\mathbf{k},1), \tag{B4}$$

we find that the symmetrized unitaries satisfy

$$\begin{aligned}\theta U_S(\mathbf{k},t)\theta^{-1} &= \theta U\left(\mathbf{k},\frac{1+t}{2}\right)\theta^{-1}\theta\left[U\left(\mathbf{k},\frac{1-t}{2}\right)\right]^\dagger\theta^{-1}\\ &= U^*\left(-\mathbf{k},\frac{1-t}{2}\right)U^{\dagger *}(-\mathbf{k},1)\\ &\quad\times\left[U^*\left(-\mathbf{k},\frac{1+t}{2}\right)U^{\dagger *}(-\mathbf{k},1)\right]^\dagger\\ &= U^*\left(-\mathbf{k},\frac{1-t}{2}\right)\left[U^*\left(-\mathbf{k},\frac{1+t}{2}\right)\right]^\dagger\\ &= U_S^*(-\mathbf{k},-t).\end{aligned} \tag{B5}$$

Then, using the properties of symmetrized unitaries, this becomes

$$\theta U_S(\mathbf{k},t)\theta^{-1} = U_S^*(-\mathbf{k},-t) = U_S^{\dagger *}(-\mathbf{k},t). \tag{B6}$$

3. Chiral symmetry

Starting from the unitary CS relation

$$CU(\mathbf{k},t)C^{-1} = U(\mathbf{k},1-t)U^\dagger(\mathbf{k},1), \tag{B7}$$

we find

$$\begin{aligned}CU_S(\mathbf{k},t)C^{-1} &= CU\left(\mathbf{k},\frac{1+t}{2}\right)C^{-1}C\left[U\left(\mathbf{k},\frac{1-t}{2}\right)\right]^\dagger C^{-1}\\ &= U\left(\mathbf{k},\frac{1-t}{2}\right)U^\dagger(\mathbf{k},1)\left[U\left(\mathbf{k},\frac{1+t}{2}\right)U^\dagger(\mathbf{k},1)\right]^\dagger\\ &= U\left(\mathbf{k},\frac{1-t}{2}\right)\left[U\left(\mathbf{k},\frac{1+t}{2}\right)\right]^\dagger\\ &= U_S(\mathbf{k},-t).\end{aligned} \tag{B8}$$

Then, again using the properties of symmetrized unitaries, we obtain

$$CU_S(\mathbf{k},t)C^{-1} = U_S(\mathbf{k},-t) = U_S^\dagger(\mathbf{k},t). \tag{B9}$$

APPENDIX C: DECOMPOSITION OF UNITARIES

In this Appendix, we prove the unitary decomposition theorem given in Sec. III, which is reproduced below.

Theorem C.1. Every unitary $U \in \mathcal{U}^S_{0,\pi}$ can be continuously deformed to a composition of a unitary loop L and a constant Hamiltonian evolution C, which we write as $U \approx L * C$. L and C are unique up to homotopy.

The proof of this theorem has two stages. First, we show that there exists a decomposition $U \approx L * C$:

Lemma C.1. Every unitary $U \in \mathcal{U}^S_{0,\pi}$ is homotopic to a product $L * C$, where L is a unitary loop and C is a constant evolution due to some static Hamiltonian (which is gapped at zero).

Proof. Let H_F be the (unique) Floquet Hamiltonian for U and let $C_\pm(s)$ be the constant evolution unitaries corresponding to the static Hamiltonians $\pm sH_F$. Consider the continuous family of unitaries

$$h(s) = [U * C_-(s)] * C_+(s). \tag{C1}$$

It is clear that $h(0)$ is homotopic to U and $h(1)$ is of the form $L * C_+(1)$ with $L = U * C_-(1)$. The endpoint of $U * C_-(1)$ is $U(1)\exp(iH_F) = \mathbb{I}$. ■

Secondly, we show that the factors L and C involved in a decomposition $L * C$ are unique up to homotopy:

Lemma C.2. Two compositions satisfy $L_1 * C_1 \approx L_2 * C_2$ if and only if $L_1 \approx L_2$ and $C_1 \approx C_2$.

Proof. $L_1 * C_1 \approx L_2 * C_2$ implies there is some function $h(s)$ for $s \in [0,1]$ such that $h(s)$ preserves the gap structure for all values of s and

$$h(0) = L_1 * C_1, \qquad h(1) = L_2 * C_2. \tag{C2}$$

Let $H(s)$ be the Floquet Hamiltonian corresponding to the unitary $h(s)$. $H(s)$ then provides a homotopy between the Floquet Hamiltonians of C_1 and C_2.

Let $C_+(s)$ be the constant evolution unitary corresponding to the Hamiltonian $H(s)$. Since $H(s)$ is independent of time, $C_+(s)$ is a constant evolution unitary that continuously interpolates between $C_+(0) = C_1$ and $C_+(1) = C_2$. Thus, $C_1 \approx C_2$.

Now, let $g(s) = h(s) * C_-(s)$, where $C_-(s)$ is the constant Hamiltonian unitary with Hamiltonian $-H(s)$. $g(s)$ is a loop for all s and interpolates between L_1 and L_2. Thus, $L_1 \approx L_2$. The proof in the reverse direction follows trivially from the definition of homotopy. ■

APPENDIX D: PROOF OF ONE-TO-ONE MAPPING BETWEEN UNITARIES AND HERMITIAN MAPS

In this section, we prove the one-to-one correspondence between unitary evolutions and Hermitian maps defined according to Eq. 15. We give the proof for the case of PHS only but note that the method may easily be extended to other symmetry classes.

Claim D.1. There is a one-to-one mapping between the set of Hermitian matrix maps that satisfy

$$P_1 H_U(\mathbf{k},t)P_1^{-1} = -H_U^*(-\mathbf{k},t) \tag{D1}$$

$$P_2 H_U(\mathbf{k},t)P_2^{-1} = H_U^*(-\mathbf{k},t) \tag{D2}$$

$$H_U^2 = \mathbb{I} \tag{D3}$$

and the set of unitary maps that satisfy $PU(\mathbf{k},t)P^{-1} = U^*(-\mathbf{k},t)$.

Proof. For a given $U(\mathbf{k},t)$, such that $PU(\mathbf{k},t)P^{-1} = U^*(-\mathbf{k},t)$, let

$$H_U = \begin{pmatrix} 0 & U(\mathbf{k},t) \\ U^\dagger(\mathbf{k},t) & 0 \end{pmatrix} \tag{D4}$$

Then, with P_1 and P_2 as defined above, it is clear that Eqs. (D1)–(D3) are satisfied.

Conversely, for a given $H_U(\mathbf{k},t)$ that satisfies Eqs. (D1) and (D2), we note that

$$P_1P_2H_U(\mathbf{k},t)(P_1P_2)^{-1} = -H_U(\mathbf{k},t) \tag{D5}$$

with

$$P_1 P_2 = \begin{pmatrix} \mathbb{I} & 0 \\ 0 & -\mathbb{I} \end{pmatrix} \tag{D6}$$

for Class D, where $P^2 = \mathbb{I}$, and

$$P_1 P_2 = \begin{pmatrix} -\mathbb{I} & 0 \\ 0 & \mathbb{I} \end{pmatrix} \tag{D7}$$

for class D, where $P^2 = -\mathbb{I}$. If

$$H_U = \begin{pmatrix} A & B \\ B^\dagger & D \end{pmatrix}, \tag{D8}$$

then Eq. (D5) implies $A = D = 0$, and Eq. (D3) implies $BB^\dagger = \mathbb{I}$, so that B is unitary. We can then write

$$H_U = \begin{pmatrix} 0 & U(\mathbf{k},t) \\ U^\dagger(\mathbf{k},t) & 0 \end{pmatrix}, \tag{D9}$$

and from Eq. (D1) we see that $PU(\mathbf{k},t)P^{-1} = U^*(-\mathbf{k},t)$. ■

APPENDIX E: ADDITIONAL K-THEORY DETAILS

In this Appendix, we give some additional details of the K-theory classification scheme outlined in the main text. For further information, we refer the reader to Refs. [10,64,65].

1. Grothendieck group of unitary maps in a symmetry class

We consider the problem of classifying unitary maps on a manifold M (for instance, $M = S^1 \times S^1$ for a periodic unitary in 1D) in a general AZ symmetry class denoted by $\mathcal{S}$. We construct a group as follows: We take pairs (U_1, U_2) and consider the operation '+' defined through

$$(U_1, U_2) + (U_3, U_4) = (U_1 \oplus U_3, U_2 \oplus U_4), \tag{E1}$$

where $\oplus$ is the direct sum. We define the equivalence of pairs in the usual (stable homotopy) sense and choose symmetry operators in such a way that a symmetry operator for the unitary $U_1 \oplus U_3$ is the tensor sum of the corresponding symmetry operators for U_1 and U_3. The pairs then form an Abelian group under $+$, where the trivial element consists of the equivalence class of pairs of the form (U, U). We denote this group by $K_U(\mathcal{S}, M)$.

2. Categories and K theory for classification of unitaries

In the main text we noted that the problem of classifying unitaries in symmetry class $\mathcal{S}$ is equivalent to the problem of classifying Hermitian maps (or 'Hamiltonians') in some enhanced symmetry class $\mathcal{S}'$. Using the same reasoning as above, we can define an Abelian group of pairs of these Hamiltonians under the '+' operation, which we write as $K(\mathcal{S}', M)$.

Following Karoubi [65], for an arbitrary Banach category, $\mathscr{C}$, let us denote by $\mathscr{C}^{p,q}$ the category whose objects are the pairs (E, ρ), where $E \in \mathrm{Ob}(\mathscr{C})$ and $\rho : C^{p,q} \to \mathrm{End}(E)$ is a K-algebra homomorphism, and where K is $\mathbb{R}$ or $\mathbb{C}$ and $C^{p,q}$ is a real or complex Clifford algebra with p negative generators and q positive generators. A morphism from the pair (E, ρ) to the pair (E', ρ') is defined to be a $\mathscr{C}$ morphism $f : E \to E'$ such that $f \cdot \rho(\lambda) = \rho(\lambda) \cdot f$ for each element λ of $C^{p,q}$.

To classify the Hamiltonians above, we now construct for every symmetry group $\mathcal{S}'$ two additive categories of the form $\mathscr{C}^{p,q}$ and $\mathscr{C}^{p',q'}$, where p, q, p', q' all depend on $\mathcal{S}'$. Here, $\mathscr{C}$ is a category which is either the category of *Real* or complex vector bundles on M, or a closely related category (depending on $\mathcal{S}'$) [80]. If $\{S_i\}$ is the set of symmetry operators corresponding to $\mathcal{S}'$, then the canonical inclusion map from $\{S_i\}$ to $\{S_i, H\}$ leads to a quasisurjective Banach functor $\phi' : \mathscr{C}^{p',q'} \to \mathscr{C}^{p,q}$. This allows us to define a Grothendieck group $K(\phi')$ associated with this functor, such that the Grothendieck group $K(\mathcal{S}', M)$ is the same as $K(\phi')$.

The canonical inclusion map $\mathscr{C}^{p,q} \subset \mathscr{C}^{p,q+1}$ induces a quasisurjective Banach functor $\phi : \mathscr{C}^{p,q+1} \longrightarrow \mathscr{C}^{p,q}$. When $\mathscr{C}$ is the category of complex vector bundles on M, then the Grothendieck group $K(\phi)$ is denoted by $K^{p,q}(M)$, and when $\mathscr{C}$ is the category of *Real* vector bundles over the *real* space M [66], then the Grothendieck group $K(\phi)$ is denoted by $KR^{p,q}(M)$. Here, the *real* space M corresponds to the existence of an involution which derives from $\mathbf{k} \to -\mathbf{k}$.

Using, repeatedly if necessary, the canonical Morita equivalences of the categories $\mathscr{C}^{p,q}$ with $\mathscr{C}^{p+1,q+1}$, and $\mathscr{C}^{p,0}$ with $\mathscr{C}^{0,p+2}$, we can establish equivalences between the categories $\mathscr{C}^{p,q}$ and $\mathscr{C}^{p',q'}$ for an arbitrary symmetry class $\mathcal{S}'$ and a category of the form $\tilde{\mathscr{C}}^{p,q}$, where $\tilde{\mathscr{C}}$ is the category of complex vector bundles over M for $\mathcal{S}' \in \{\mathrm{A}, \mathrm{AIII}\}$ and the category of *Real* vector bundles over M for all other symmetry classes. This then allows us to identify $K(\mathcal{S}', M)$ with some $KR^{0,q}(M)$ (with $0 \leqslant q < 8$) or some $K^{0,q}(M)$ (with $0 \leqslant q < 2$) and leads to the results in the main text. Further details will be presented elsewhere.

[1] M. Hasan and C. Kane, Colloquium: Topological insulators, Rev. Mod. Phys. **82**, 3045 (2010).

[2] X.-L. Qi and S.-C. Zhang, Topological insulators and superconductors, Rev. Mod. Phys. **83**, 1057 (2011).

[3] C. L. Kane and E. J. Mele, Quantum Spin Hall Effect in Graphene, Phys. Rev. Lett. **95**, 226801 (2005).

[4] J. E. Moore and L. Balents, Topological invariants of time-reversal-invariant band structures, Phys. Rev. B **75**, 121306 (2007).

[5] R. Roy, Topological phases and the quantum spin Hall effect in three dimensions, Phys. Rev. B **79**, 195322 (2009).

[6] L. Fu, C. L. Kane, and E. J. Mele, Topological Insulators in Three Dimensions, Phys. Rev. Lett. **98**, 106803 (2007).

[7] R. Roy, Topological superfluids with time reversal symmetry, arXiv:0803.2868.

[8] R. Roy, Topological invariants of time reversal invariant superconductors, arXiv:cond-mat/0608064.

[9] A. P. Schnyder, S. Ryu, A. Furusaki, and A. W. W. Ludwig, Classification of topological insulators and superconductors in three spatial dimensions, Phys. Rev. B **78**, 195125 (2008).
[10] A. Kitaev, Periodic table for topological insulators and superconductors, in *Advances in Theoretical Physics: Landau Memorial Conference Chernogolokova (Russia)*, AIP Conf. Proc. No. 1134 (American Institute of Physics, New York, 2009), pp. 22–30.
[11] J. Cayssol, B. Dóra, F. Simon, and R. Moessner, Floquet topological insulators, Phys. Status Solidi RRL **7**, 101 (2013).
[12] M. Bukov, L. D'Alessio, and A. Polkovnikov, Universal high-frequency behavior of periodically driven systems: from dynamical stabilization to Floquet engineering, Adv. Phys. **64**, 139 (2015).
[13] W. Yao, A. H. MacDonald, and Q. Niu, Optical Control of Topological Quantum Transport in Semiconductors, Phys. Rev. Lett. **99**, 047401 (2007).
[14] T. Oka and H. Aoki, Photovoltaic Hall effect in graphene, Phys. Rev. B **79**, 081406 (2009).
[15] J.-I. Inoue and A. Tanaka, Photoinduced Transition between Conventional and Topological Insulators in Two-Dimensional Electronic Systems, Phys. Rev. Lett. **105**, 017401 (2010).
[16] N. H. Lindner, G. Refael, and V. Galitski, Floquet topological insulator in semiconductor quantum wells, Nat. Phys. **7**, 490 (2011).
[17] T. Kitagawa, T. Oka, A. Brataas, L. Fu, and E. Demler, Transport properties of nonequilibrium systems under the application of light: Photoinduced quantum Hall insulators without Landau levels, Phys. Rev. B **84**, 235108 (2011).
[18] N. H. Lindner, D. L. Bergman, G. Refael, and V. Galitski, Topological Floquet spectrum in three dimensions via a two-photon resonance, Phys. Rev. B **87**, 235131 (2013).
[19] A. G. Grushin, Á. Gómez-León, and T. Neupert, Floquet Fractional Chern Insulators, Phys. Rev. Lett. **112**, 156801 (2014).
[20] P. M. Perez-Piskunow, G. Usaj, C. A. Balseiro, and L. E. F. F. Torres, Floquet chiral edge states in graphene, Phys. Rev. B **89**, 121401 (2014).
[21] L. E. F. Foa Torres, P. M. Perez-Piskunow, C. A. Balseiro, and G. Usaj, Multiterminal Conductance of a Floquet Topological Insulator, Phys. Rev. Lett. **113**, 266801 (2014).
[22] H. L. Calvo, L. E. F. Foa Torres, P. M. Perez-Piskunow, C. A. Balseiro, and G. Usaj, Floquet interface states in illuminated three-dimensional topological insulators, Phys. Rev. B **91**, 241404 (2015).
[23] T. Iadecola, L. H. Santos, and C. Chamon, Stroboscopic symmetry-protected topological phases, Phys. Rev. B **92**, 125107 (2015).
[24] T. Kitagawa, M. A. Broome, A. Fedrizzi, and M. S. Rudner, Observation of topologically protected bound states in photonic quantum walks, Nat. Commun. **3**, 882 (2012).
[25] M. C. Rechtsman, J. M. Zeuner, Y. Plotnik, Y. Lumer, D. Podolsky, F. Dreisow, S. Nolte, M. Segev, and A. Szameit, Photonic Floquet topological insulators, Nature (London) **496**, 196 (2013).
[26] L. J. Maczewsky, J. M. Zeuner, S. Nolte, and A. Szameit, Observation of photonic anomalous Floquet topological insulators, Nat. Commun. **8**, 13756 (2017).
[27] F. Cardano, A. D'Errico, A. Dauphin, M. Maffei, B. Piccirillo, C. de Lisio, G. De Filippis, V. Cataudella, E. Santamato, L. Marrucci, M. Lewenstein, and P. Massignan, Detection of Zak phases and topological invariants in a chiral quantum walk of twisted photons, Nat. Commun. **8**, 15516 (2017).
[28] G. Jotzu, M. Messer, R. Desbuquois, and M. Lebrat, Experimental realization of the topological Haldane model with ultracold fermions, Nature (London) **515**, 237 (2014).
[29] K. Jiménez-García, L. J. LeBlanc, R. A. Williams, M. C. Beeler, C. Qu, M. Gong, C. Zhang, and I. B. Spielman, Tunable Spin-Orbit Coupling via Strong Driving in Ultracold-Atom Systems, Phys. Rev. Lett. **114**, 125301 (2015).
[30] Y. H. Wang, H. Steinberg, P. Jarillo-Herrero, and N. Gedik, Observation of Floquet-Bloch states on the surface of a topological insulator, Science **342**, 453 (2013).
[31] B. M. Fregoso, Y. H. Wang, N. Gedik, and V. Galitski, Driven electronic states at the surface of a topological insulator, Phys. Rev. B **88**, 155129 (2013).
[32] T. Kitagawa, E. Berg, M. Rudner, and E. Demler, Topological characterization of periodically driven quantum systems, Phys. Rev. B **82**, 235114 (2010).
[33] L. Jiang, T. Kitagawa, J. Alicea, A. R. Akhmerov, D. Pekker, G. Refael, J. I. Cirac, E. Demler, M. D. Lukin, and P. Zoller, Majorana Fermions in Equilibrium and in Driven Cold-Atom Quantum Wires, Phys. Rev. Lett. **106**, 220402 (2011).
[34] M. S. Rudner, N. H. Lindner, E. Berg, and M. Levin, Anomalous Edge States and the Bulk-Edge Correspondence for Periodically Driven Two-Dimensional Systems, Phys. Rev. X **3**, 031005 (2013).
[35] M. Thakurathi, A. A. Patel, D. Sen, and A. Dutta, Floquet generation of Majorana end modes and topological invariants, Phys. Rev. B **88**, 155133 (2013).
[36] J. K. Asbóth, B. Tarasinski, and P. Delplace, Chiral symmetry and bulk-boundary correspondence in periodically driven one-dimensional systems, Phys. Rev. B **90**, 125143 (2014).
[37] P. Titum, E. Berg, M. S. Rudner, G. Refael, and N. H. Lindner, Anomalous Floquet-Anderson Insulator as a Nonadiabatic Quantized Charge Pump, Phys. Rev. X **6**, 021013 (2016).
[38] F. Nathan and M. S. Rudner, Topological singularities and the general classification of Floquet–Bloch systems, New J. Phys. **17**, 125014 (2015).
[39] D. Carpentier, P. Delplace, M. Fruchart, and K. Gawedzki, Topological Index for Periodically Driven Time-Reversal Invariant 2D Systems, Phys. Rev. Lett. **114**, 106806 (2015).
[40] P. Titum, N. H. Lindner, M. C. Rechtsman, and G. Refael, Disorder-Induced Floquet Topological Insulators, Phys. Rev. Lett. **114**, 056801 (2015).
[41] M. Fruchart, Complex classes of periodically driven topological lattice systems, Phys. Rev. B **93**, 115429 (2016).
[42] J. K. Asbóth, Symmetries, topological phases, and bound states in the one-dimensional quantum walk, Phys. Rev. B **86**, 195414 (2012).
[43] J. K. Asboth and H. Obuse, Bulk-boundary correspondence for chiral symmetric quantum walks, Phys. Rev. B **88**, 121406 (2013).
[44] B. Tarasinski, J. K. Asbóth, and J. P. Dahlhaus, Scattering theory of topological phases in discrete-time quantum walks, Phys. Rev. A **89**, 042327 (2014).
[45] T. Rakovszky and J. K. Asboth, Localization, delocalization, and topological phase transitions in the one-dimensional split-step quantum walk, Phys. Rev. A **92**, 052311 (2015).
[46] D. J. Thouless, Quantization of particle transport, Phys. Rev. B **27**, 6083 (1983).

[47] L. Fu and C. L. Kane, Time reversal polarization and a Z_2 adiabatic spin pump, Phys. Rev. B **74**, 195312 (2006).
[48] R. Roy, Topological pumps and adiabatic cycles, arXiv:1104.1979.
[49] J. C. Y. Teo and C. L. Kane, Topological defects and gapless modes in insulators and superconductors, Phys. Rev. B **82**, 115120 (2010).
[50] F. Zhang and C. L. Kane, Anomalous topological pumps and fractional Josephson effects, Phys. Rev. B **90**, 020501 (2014).
[51] D. V. Else and C. Nayak, Classification of topological phases in periodically driven interacting systems, Phys. Rev. B **93**, 201103 (2016).
[52] A. C. Potter, T. Morimoto, and A. Vishwanath, Classification of Interacting Topological Floquet Phases in One Dimension, Phys. Rev. X **6**, 041001 (2016).
[53] C. W. von Keyserlingk and S. L. Sondhi, Phase structure of one-dimensional interacting Floquet systems. I. Abelian symmetry-protected topological phases, Phys. Rev. B **93**, 245145 (2016).
[54] R. Roy and F. Harper, Abelian Floquet symmetry-protected topological phases in one dimension, Phys. Rev. B **94**, 125105 (2016).
[55] H. C. Po, L. Fidkowski, T. Morimoto, and A. C. Potter, Chiral Floquet Phases of Many-body Localized Bosons, Phys. Rev. X **6**, 041070 (2016).
[56] F. Harper and R. Roy, Floquet Topological Order in Interacting Systems of Bosons and Fermions, Phys. Rev. Lett. **118**, 115301 (2017).
[57] A. C. Potter and T. Morimoto, Dynamically enriched topological orders in driven two-dimensional systems, Phys. Rev. B **95**, 155126 (2017).
[58] R. Roy and F. Harper, Floquet topological phases with symmetry in all dimensions, Phys. Rev. B **95**, 195128 (2017).
[59] P. Heinzner, A. Huckleberry, and M. R. Zirnbauer, Symmetry classes of disordered fermions, Commun. Math. Phys. **257**, 725 (2005).
[60] A. Altland and M. R. Zirnbauer, Nonstandard symmetry classes in mesoscopic normal-superconducting hybrid structures, Phys. Rev. B **55**, 1142 (1997).
[61] M. R. Zirnbauer, Riemannian symmetric superspaces and their origin in random-matrix theory, J. Math. Phys. **37**, 4986 (1996).
[62] More general definitions may be used, but this definition suffices to capture the interesting aspects of the problem.
[63] M. Nakahara, *Geometry, Topology and Physics, Second Edition*, Graduate Student Series in Physics (Taylor and Francis, New York, 2003).
[64] M. F. Atiyah, *K-Theory* (Benjamin, New York, NY, 1967).
[65] M. Karoubi, *K-Theory: An Introduction*, Classics in Mathematics (Springer, Berlin, 1978).
[66] M. F. Atiyah, *K*-theory and reality, Q. J. Math. **17**, 367 (1966).
[67] D. V. Else, B. Bauer, and C. Nayak, Floquet Time Crystals, Phys. Rev. Lett. **117**, 090402 (2016).
[68] A. Lazarides, A. Das, and R. Moessner, Equilibrium states of generic quantum systems subject to periodic driving, Phys. Rev. E **90**, 012110 (2014).
[69] L. D'Alessio and M. Rigol, Long-time Behavior of Isolated Periodically Driven Interacting Lattice Systems, Phys. Rev. X **4**, 041048 (2014).
[70] P. Ponte, A. Chandran, Z. Papic, and D. A. Abanin, Periodically driven ergodic and many-body localized quantum systems, Ann. Phys. **353**, 196 (2015).
[71] L. D'Alessio and A. Polkovnikov, Many-body energy localization transition in periodically driven systems, Ann. Phys. **333**, 19 (2013).
[72] P. Ponte, Z. Papic, F. Huveneers, and D. A. Abanin, Many-Body Localization in Periodically Driven Systems, Phys. Rev. Lett. **114**, 140401 (2015).
[73] A. Lazarides, A. Das, and R. Moessner, Fate of Many-Body Localization Under Periodic Driving, Phys. Rev. Lett. **115**, 030402 (2015).
[74] D. A. Abanin, W. De Roeck, and F. Huveneers, Exponentially Slow Heating in Periodically Driven Many-Body Systems, Phys. Rev. Lett. **115**, 256803 (2015).
[75] D. A. Abanin, W. De Roeck, and F. Huveneers, Theory of many-body localization in periodically driven systems, Ann. Phys. **372**, 1 (2016).
[76] L. Zhang, V. Khemani, and D. A. Huse, A Floquet model for the many-body localization transition, Phys. Rev. B **94**, 224202 (2016).
[77] R. Nandkishore and D. A. Huse, Many-body localization and thermalization in quantum statistical mechanics, Ann. Rev. Condens. Matter Phys. **6**, 15 (2015).
[78] W. De Roeck and F. Huveneers, Stability and instability towards delocalization in many-body localization systems, Phys. Rev. B **95**, 155129 (2017).
[79] K. Agarwal, E. Altman, E. Demler, S. Gopalakrishnan, D. A. Huse, and M. Knap, Rare-region effects and dynamics near the many-body localization transition, Ann. Phys. **529**, 1600326 (2017).
[80] For definitions see Ref. [65].